Joint Frequency-Domain Differential Detection and Equalization for DS-CDMA Signal Transmissions in a Frequency-Selective Fading Channel

Le Liu, *Student Member, IEEE,* and Fumiyuki Adachi, *Fellow, IEEE*

***Abstract*—It has been revealed that direct sequence code-division multiple access (DS-CDMA) can achieve a good bit-error rate (BER) performance, comparable to multicarrier CDMA (MC-CDMA), by using coherent frequency-domain equalization (FDE) instead of coherent Rake combining. However, coherent FDE requires accurate channel estimation. Pilot-assisted channel estimation is a practical solution, but its accuracy is sensitive to the Doppler spread. In this paper, a frequency-domain differential encoding and detection scheme is proposed for a DS-CDMA mobile radio. Joint frequency-domain differential detection and equalization (FDDDE) based on minimum mean-square error (MMSE) criterion is presented, where a simple decision feedback filter is used to provide a reliable reference signal for MMSE-FDDDE. Also presented is an approximate BER analysis. It is confirmed by both approximate BER analysis and computer simulation that MMSE-FDDDE provides good BER performance close to the coherent MMSE-FDE and shows high robustness against the Doppler spread; it outperforms coherent MMSE-FDE for large Doppler spreads. The proposed MMSE-FDDDE can also be applied to MC-CDMA. A performance comparison between uncoded DS- and MC-CDMA shows that DS-CDMA with MMSE-FDDDE achieves better BER performance than MC-CDMA with MMSE-FDDDE for small spreading factors.**

***Index Terms*—Direct sequence code-division multiple access (DS-CDMA), frequency-domain differential detection (FDDD), frequency-domain equalization (FDE).**

I. Introduction

THE INCREASING demand for broadband services requires future wireless communication systems to support very high transmission rates of up to nearly 100 Mb/s [1]. However, the frequency-selective multipath fading, encountered in a broadband wireless communication system, severely degrades the bit-error rate (BER) performance [2],[3]. In direct sequence code-division multiple-access systems (DS-CDMA) [4], coherent Rake combining can exploit the channel frequency-selectivity through the path-diversity effect to improve the BER performance [5]. However, due to an excessive number of resolvable multiple paths in a broadband wireless channel, the complexity of coherent Rake combining increases greatly; furthermore, the BER performance degrades because a severe interpath interference (IPI) offsets the obtainable path-diversity effect by using coherent Rake combining [5]. Recently, multicarrier CDMA (MC-CDMA) [6]–[9], which is the combination of orthogonal frequency-division multiplexing (OFDM) and CDMA, has been attracting much attention. In MC-CDMA, the data symbol to be transmitted is spread over a number of subcarriers; hence, the frequency-diversity gain can be attained by using coherent frequency-domain equalization (FDE) [9].

Quite recently, coherent FDE has drawn a lot of interest in single-carrier wireless transmission [10]. DS-CDMA is a family of the single-carrier transmission (DS-CDMA is sometimes called single-carrier CDMA) and FDE can also be applied to it. It has been found [11] that coherent FDE is more effective than coherent Rake combining for the reception of DS-CDMA signals in a frequency-selective fading channel. Both the theoretical analysis and computer simulations have shown [12] that coherent FDE based on minimum mean-square error (MMSE) criterion provides the best BER performance among zero forcing (ZF), maximal ratio combing (MRC), and MMSE [13]. The complexity of a coherent MMSE-FDE receiver is independent of the channel frequency selectivity, unlike that of the coherent Rake receiver; the use of coherent FDE can alleviate the complexity problem of the coherent Rake receiver, arising from too many paths in a severe frequency-selective fading channel. Coherent MMSE-FDE requires accurate channel estimation. However, in practical wireless communication systems, the BER performance suffers from channel estimation errors. Several pilot-assisted channel estimation schemes have been proposed so far for coherent FDE in the reception of MC- and DS-CDMA signals [14]–[16], where the known pilot block is periodically transmitted. In order to acquire better tracking ability against fast fading, the pilot block transmission rate has to be increased, but this results in the loss of transmission efficiency. For applications like mobile radio, differential detection is sometimes preferable because of its simple implementation due to no requirement of channel estimation, but differential detection is inferior to that of coherent detection since a delayed version of the received noisy signal is used as the phase reference. However, in a fast-fading channel, differential detection is more attractive, where coherent detection becomes practically infeasible.

In this paper, a frequency-domain differential encoding and detection scheme is proposed for DS-CDMA mobile radio. Joint frequency-domain differential detection and equalization (FDDDE) is presented. A simple decision feedback filtering is used to provide the noise-reduced reference signal. The

Manuscript received January 16, 2005; revised May 2, 2005.

The authors are with the Adachi Laboratory, Department of Electrical and Communication Engineering, Graduate School of Engineering, Tohoku University, Sendai 980-8580, Japan (e-mail: liule@mobile.ecei.tohoku.ac.jp; adachi@ecei.tohoku.ac.jp).

Digital Object Identifier 10.1109/JSAC.2005.862416

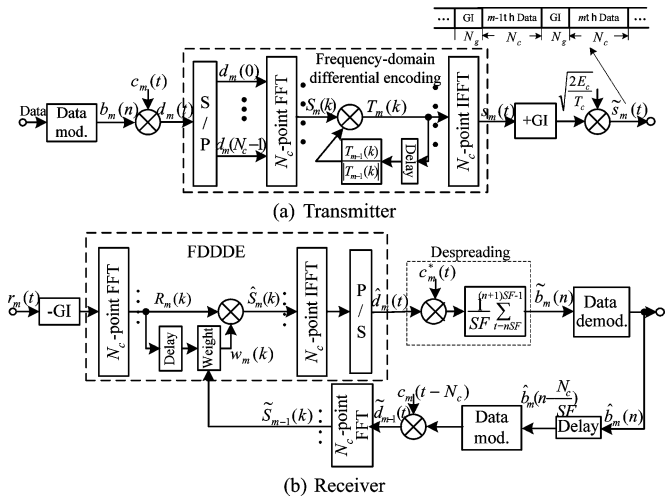

Fig. 1. Transmission structure of DS-CDMA system with FDDDE.

achievable BER performance of the proposed FDDDE is evaluated by computer simulation and is compared with that of coherent FDE in DS-CDMA. An approximate BER analysis is also presented. Coding, while desirable, is not necessary for combating frequency selectivity [17]. Therefore, in this paper, we focus on the uncoded case in order to show the potential performance of DS-CDMA using FDDDE in a frequency-selective fading channel. The proposed FDDDE can also be applied to MC-CDMA. A performance comparison between uncoded DS- and MC-CDMA, both using FDDDE, is presented.

The remainder of this paper is organized as follows. Section II presents the transmission system model of DS-CDMA using FDDDE. Then, MMSE and ZF equalization weights are derived for FDDDE in Section III. An expression for the approximate conditional BER for the given set of channel gains is derived. Using the derived conditional BER expression, the approximate average BER is evaluated by the Monte Carlo numerical computation method in Section IV, which is confirmed by computer simulation. A performance comparison between uncoded DS- and MC-CDMA is also presented in Section IV. Section V offers concluding remarks and future work.

II. System Model

The DS-CDMA transmission system model is illustrated in Fig. 1. We consider block transmissions of N_c chips, where N_c is the fast Fourier transform (FFT) block length for frequency-domain differential encoding. At a transmitter, the nth data-modulated symbol $b_m(n)$ to be transmitted during the mth block is spread by the spreading sequence $c_m(t)$, with $|b_m(n)| = |c_m(t)| = 1$. The resultant mth block spread chip sequence $d_m(t)$ can be expressed as

$$d_m(t) = b_m\left(\left\lfloor \frac{t}{SF} \right\rfloor\right) c_m(t) \tag{1}$$

for $t = 0 \sim (N_c - 1)$, where *SF* is the spreading factor and $\lfloor x \rfloor$ is the largest integer smaller than or equal to x. Then, the N_c-point FFT is applied to decompose the mth block chip sequence into N_c subcarrier components (hereafter, we use the terminology "subcarrier" instead of the frequency component). The kth subcarrier component of the mth chip block is given by

$$S_m(k) = \frac{1}{\sqrt{N_c}} \sum_{t=0}^{N_c-1} d_m(t) \exp\left(-j2\pi k \frac{t}{N_c}\right) \tag{2}$$

for $k = 0 \sim (N_c - 1)$. If $c_m(t)$ is a random chip sequence, $S_m(k)$ is also a random variable with zero mean and unity variance

$$E[|S_m(k)|^2] = 1 \tag{3}$$

where $E[.]$ is the ensemble average operation. Block-by-block frequency-domain differential encoding at the kth subcarrier is performed as follows:

$$T_m(k) = S_m(k) \frac{T_{m-1}(k)}{|T_{m-1}(k)|} \tag{4}$$

with $m \geq 1$, where $T_m(k)$ is the differentially encoded subcarrier component with $|T_m(k)| = |S_m(k)|$. At $m = 0$, the reference (or pilot) chip block known to a receiver needs to be transmitted; $T_0(k)$ is the kth subcarrier component of the known reference chip sequence. Then, the N_c-point IFFT is applied to obtain the mth block differentially encoded DS-CDMA signal in the time domain, which can be expressed as

$$s_m(t) = \frac{1}{\sqrt{N_c}} \sum_{k=0}^{N_c-1} T_m(k) \exp\left(j2\pi t \frac{k}{N_c}\right) \tag{5}$$

for $t = 0 \sim (N_c - 1)$. In order to apply FFT at the receiver, it is necessary to insert the guard interval (GI) of N_g chips at the beginning of each block, similarly to MC-CDMA [10]. The GI-inserted chip sequence of the mth block can be expressed as

$$\tilde{s}_m(t) = \sqrt{\frac{2E_c}{T_c}} s_m(t) \tag{6}$$

for $t = -N_g \sim (N_c - 1)$, where E_c is the average chip energy and T_c is chip duration.

In this paper, we assume the square-root Nyquist chip-shaping filter at the transmitter and the same filter at the receiver as the chip-matched filter. Ideal chip sampling time is assumed at the receiver. Therefore, the chip-spaced discrete-time signal representation is used throughout the paper. Also assumed is a block-fading channel having L independent propagation paths with chip-spaced time delays, $\{\tau_l; l = 0 \sim (L-1)\}$, which means that the path gains remain constant over the one-block interval of $(N_c + N_g)$ chips, but they vary block by block according to the terminal movement. Also, the maximum time delay of the channel is assumed to be shorter than GI, i.e., $\max_l\{\tau_l\} \leq (N_g - 1)$. The channel impulse response for the reception of the mth block can be expressed as [18]

$$h_m(t) = \sum_{l=0}^{L-1} h_{m,l} \delta(t - \tau_l) \tag{7}$$

where $\delta(x)$ is the delta function and $h_{m,l}$ is the lth path gain with $E[\sum_{l=0}^{L} |h_{m,l}|^2] = 1$.

The received signal is sampled at the chip rate to obtain [12]

$$r_m(t) = \sum_{l=0}^{L-1} h_{m,l}\widetilde{s}_m(t-\tau_l) + \eta_m(t) \tag{8}$$

where $\eta_m(t)$ is the additive white Gaussian noise (AWGN) process with zero mean and a variance of $2N_0/T_c$ (N_0 being the single-sided power spectrum density). As shown in Fig. 1(b), after removal of GI, the N_c-point FFT is applied and the received signal sequence $r_m(t)$ is decomposed into N_c subcarrier components

$$\begin{aligned} R_m(k) &= \frac{1}{\sqrt{N_c}} \sum_{t=0}^{N_c-1} r_m(t) \exp\left(-j2\pi k \frac{t}{N_c}\right) \\ &= \sqrt{\frac{2E_c}{T_c}} T_m(k) H_m(k) + \Pi_m(k) \end{aligned} \tag{9}$$

where $H_m(k)$ is the channel gain at the kth subcarrier with $E[|H_m(k)|^2] = 1$ and $\Pi_m(k)$ is the noise component with zero-mean and a variance of $E[|\Pi_m(k)|^2] = 2N_0/T_c$ [3]. They are given by

$$\begin{cases} H_m(k) = \sum\limits_{l=0}^{L-1} h_{m,l} \exp\left(-j2\pi k \frac{\tau_l}{N_c}\right) \\ \Pi_m(k) = \frac{1}{\sqrt{N_c}} \sum\limits_{t=0}^{N_c-1} \eta_m(t) \exp\left(-j2\pi k \frac{t}{N_c}\right) \end{cases}. \tag{10}$$

Subcarrier-by-subcarrier FDDDE is performed as

$$\hat{S}_m(k) = w_m(k) R_m(k) \tag{11}$$

where $w_m(k)$ acts as the reference signal for differential detection as well as an equalization weight, which is derived in Section III. Then, the N_c-point IFFT is applied to obtain the time-domain chip sequence

$$\hat{d}_m(t) = \frac{1}{\sqrt{N_c}} \sum_{k=0}^{N_c-1} \hat{S}_m(k) \exp\left(j2\pi t \frac{k}{N_c}\right). \tag{12}$$

Finally, despreading is carried out to get the decision variable $\hat{b}_m(n)$ for the detection of $b_m(n)$

$$\hat{b}_m(n) = \frac{1}{SF} \sum_{t=nSF}^{(n+1)SF-1} \hat{d}_m(t) c_m^*(t) \tag{13}$$

based on which data demodulation is performed to obtain $\widetilde{b}_m(n)$.

III. Derivation of FDDDE Weights

The set of FDDDE weights $\{w_m(k); k = 0 \sim (N_c - 1)\}$ is derived according to the MMSE criterion [3]. Substituting (4) and (9) into (11), $\hat{S}_m(k)$ can be expressed as

$$\begin{aligned} \hat{S}_m(k) &= w_m(k) R_m(k) \\ &= \sqrt{\frac{2E_c}{T_c}} w_m(k) H_m(k) S_m(k) \frac{T_{m-1}(k)}{|T_{m-1}(k)|} + w_m(k)\Pi_m(k). \end{aligned} \tag{14}$$

We define the equalization error for the kth subcarrier component of the mth block signal as

$$\begin{aligned} \varepsilon_m(k) &= S_m(k) - \hat{S}_m(k) \\ &= S_m(k)\left[1 - \sqrt{\frac{2E_c}{T_c}} w_m(k) H_m(k) \frac{T_{m-1}(k)}{|T_{m-1}(k)|}\right] \\ &\quad - w_m(k)\Pi_m(k). \end{aligned} \tag{15}$$

The mean-square error $E[|\varepsilon_m(k)|^2]$ for the given set of $\{H_m(k)$ and $H_{m-1}(k);\ k = 0 \sim (N_c - 1)\}$ is derived as

$$\begin{aligned} E[|\varepsilon_m(k)|^2] = &\left[1 + \left|\sqrt{\frac{2E_c}{T_c}} w_m(k) H_m(k) \frac{T_{m-1}(k)}{|T_{m-1}(k)|}\right|^2\right. \\ &\left. -2\mathrm{Re}\left\{\sqrt{\frac{2E_c}{T_c}} w_m(k) H_m(k) \frac{T_{m-1}(k)}{|T_{m-1}(k)|}\right\} + \frac{2N_0}{T_c}|w_m(k)|^2\right]. \end{aligned} \tag{16}$$

The set of weights that satisfies $\partial E[|\varepsilon_m(k)|^2]/\partial w(k) = 0$ is the optimum one in the MMSE sense [3] and is given by

$$w_m(k) = \frac{\sqrt{\frac{2E_c}{T_c}} H_m^*(k) \frac{T_{m-1}^*(k)}{|T_{m-1}(k)|}}{\left|\sqrt{\frac{2E_c}{T_c}} H_m(k) \frac{T_{m-1}(k)}{|T_{m-1}(k)|}\right|^2 + \frac{2N_0}{T_c}} \qquad \text{for MMSE.} \tag{17}$$

Similarly, we can derive the set of FDDDE weights satisfying the zero-forcing (ZF) criterion [3], that is

$$w_m(k) = \frac{\sqrt{\frac{2E_c}{T_c}} H_m^*(k) \frac{T_{m-1}^*(k)}{|T_{m-1}(k)|}}{\left|\sqrt{\frac{2E_c}{T_c}} H_m(k) \frac{T_{m-1}(k)}{|T_{m-1}(k)|}\right|^2} \qquad \text{for ZF.} \tag{18}$$

However, $\sqrt{2E_c/T_c} H_m(k) T_{m-1}(k)/|T_{m-1}(k)|$ is not known to the receiver. Assuming a very slow fading (i.e., $H_m(k) \approx H_{m-1}(k)$), we replace $\sqrt{2E_c/T_c} H_m(k) T_{m-1}(k)$ by $\sqrt{2E_c/T_c} H_{m-1}(k) T_{m-1}(k)$. From (4), we have $|T_{m-1}(k)| = |S_{m-1}(k)|$. Hence, $|T_{m-1}(k)|$ can be replaced by $\left|\widetilde{S}_{m-1}(k)\right|$, where $\widetilde{S}_{m-1}(k)$ is the kth subcarrier component of the previous chip block obtained by the feedback of $\{\widetilde{d}_{m-1}(n)\}$. Consequently, we have the following weight:

$$w_m(k) = \begin{cases} \frac{X_{m-1}^*(k)}{|X_{m-1}(k)|^2 + \frac{2N_0}{T_c}}, & \text{for MMSE} \\ \frac{X_{m-1}^*(k)}{|X_{m-1}(k)|^2}, & \text{for ZF} \end{cases} \tag{19}$$

where

$$X_{m-1}(k) = \frac{R_{m-1}(k)}{\left|\widetilde{S}_{m-1}(k)\right|}. \tag{20}$$

Since $X_{m-1}(k)$ is noisy, we apply infinite impulse response (IIR) filtering [19]–[21] with decision feedback of past chip blocks $\{\widetilde{S}_{m-k}; k = 1 \sim (m-1)\}$ [22], [23]. Using

$$\frac{T_{m-1}(k)}{|S_{m-1}(k)|} = \frac{S_{m-1}(k)}{|S_{m-1}(k)|} \frac{T_{m-2}(k)}{|S_{m-2}(k)|}$$

and $|T_{m-1}(k)| = |S_{m-1}(k)|$ from (4), we have

$$\hat{X}_{m-1}(k) = \alpha \hat{X}_{m-2}(k) \frac{\widetilde{S}_{m-1}(k)}{\left|\widetilde{S}_{m-1}(k)\right|} + (1-\alpha) X_{m-1}(k) \quad (21)$$

for $m \geq 2$, where α ($0 \leq \alpha \leq 1$) is the forgetting factor. $X_{m-1}(k)$ in (19) is replaced by the filter output $\hat{X}_{m-1}(k)$ to improve the reliability of the FDDDE weight. In (21), $\hat{X}_0(k) = \mathrm{X}_0(k) = R_0(k)/|T_0(k)|$, where $R_0(k)$ is the kth subcarrier component of the received reference signal. The FDDDE weight using decision feedback IIR filtering can be given by

$$w_m(k) = \begin{cases} \dfrac{\hat{X}^*_{m-1}(k)}{\left|\hat{X}_{m-1}(k)\right|^2 + \frac{2N_0}{T_c}}, & \text{for MMSE-FDDDE} \\ \dfrac{\hat{X}^*_{m-1}(k)}{\left|\hat{X}_{m-1}(k)\right|^2}, & \text{for ZF-FDDDE} \end{cases} . \quad (22)$$

α is an important design parameter to determine the tracking ability against fading [22]. The optimum value of α depends on the channel condition. By letting $\alpha \to 1$, the noise contribution can be sufficiently suppressed, but the tracking ability against fading tends to be lost. As the fading becomes faster, α should be smaller to better track the fading variations. The noise reduction and fading tracking ability are in a tradeoff relationship. Assuming a very slow fading (i.e., $H_{m-1}(k) = H_{m-2}(k) = H_{m-3}(k) \ldots$) and perfect decision feedback (the decision error probability is negligible), we have

$$\begin{aligned} \hat{X}_{m-1}(k) &\overset{\alpha \to 1}{\to} \sqrt{\frac{2E_c}{T_c}} \left(\frac{T_{m-1}(k)}{|S_{m-1}(k)|} \right) H_{m-1}(k) \\ &= \sqrt{\frac{2E_c}{T_c}} \left(\frac{T_{m-1}(k)}{|T_{m-1}(k)|} \right) H_{m-1}(k) \end{aligned} \quad (23)$$

for large m. Assuming $H_m(k) \approx H_{m-1}(k)$, we get, from (4)

$$T_m(k) H_m(k) \approx S_m(k) H_{m-1}(k) \left[\frac{T_m(k)}{T_{m-1}(k)} \right] \quad (24)$$

then we obtain, from (23)

$$\sqrt{\frac{2E_c}{T_c}} T_m(k) H_m(k) \approx S_m(k) \hat{X}_m(k). \quad (25)$$

Therefore, $S_m(k)$ can be approximated as

$$\begin{aligned} S_m(k) &\approx \sqrt{\frac{2E_c}{T_c}} T_m(k) H_m(k) \left(\frac{\hat{X}^*_m(k)}{\left|\hat{X}_m(k)\right|^2} \right) \\ &= \sqrt{\frac{2E_c}{T_c}} T_m(k) H_m(k) w_m(k) \end{aligned} \quad (26)$$

for ZF-FDDDE. This suggests that $w_m(k)$ acts as the reference signal for differential detection as well as an equalization weight.

IV. Approximate BER Analysis

The FDDDE output $\hat{S}_m(k)$, given by (11), can be rewritten as

$$\hat{S}_m(k) = \alpha_m(k) S_m(k) + \hat{\Pi}_m(k) \quad (27)$$

where

$$\begin{cases} \alpha_m(k) = \sqrt{\frac{2E_c}{T_c}} w_m(k) H_m(k) \frac{T_{m-1}(k)}{|T_{m-1}(k)|} \\ \hat{\Pi}_m(k) = w_m(k) \Pi_m(k) \end{cases} . \quad (28)$$

Substituting (27) into (12), the time-domain chip sequence obtained by the N_c-point IFFT after joint differential detection and equalization is given by

$$\begin{aligned} \hat{s}_m(t) &= \frac{1}{\sqrt{N_c}} \sum_{k=0}^{N_c-1} \hat{S}_m(k) \exp\left(j2\pi t \frac{k}{N_c} \right) \\ &= \left(\frac{1}{N_c} \sum_{k=0}^{N_c-1} \alpha_m(k) \right) s_m(t) \\ &\quad + \frac{1}{N_c} \sum_{k=0}^{N_c-1} \alpha_m(k) \left[\sum_{\substack{\tau=0 \\ \tau \neq t}}^{N_c-1} s_m(\tau) \exp\left(j2\pi k \frac{t-\tau}{N_c} \right) \right] \\ &\quad + \frac{1}{\sqrt{N_c}} \sum_{k=0}^{N_c-1} \hat{\Pi}_m(k) \exp\left(j2\pi t \frac{k}{N_c} \right) \end{aligned} \quad (29)$$

where the first term represents the desired signal component, the second is the interchip interference (ICI), and the third is the equivalent noise component. Substituting (29) into (13), the decision variable $\hat{d}_m(n)$ is given by

$$\hat{d}_m(n) = \left(\frac{1}{N_c} \sum_{k=0}^{N_c-1} \alpha_m(k) \right) d_m(n) + \mu_{\mathrm{ICI}} + \mu_{\mathrm{AWGN}} \quad (30)$$

where the first term represents the desired data symbol and the second and third terms are the ICI and the noise after despreading due to the AWGN, respectively. μ_{ICI} and μ_{AWGN} are given by (31), shown at the bottom of the page. By approximating μ_{ICI} as a zero-mean complex-valued Gaussian variable, the sum of μ_{ICI} and μ_{AWGN} can be treated as a new zero-mean complex-valued Gaussian noise μ. The variance of μ is the sum of those of μ_{ICI} and μ_{AWGN}

$$2\sigma^2_\mu = E[|\mu|^2] = 2\sigma^2_{\mathrm{ICI}} + 2\sigma^2_{\mathrm{AWGN}} \quad (32)$$

$$\begin{cases} \mu_{\mathrm{ICI}} = \frac{1}{SF} \sum_{t=nSF}^{(n+1)SF-1} \left\{ c^*_m(t) \times \frac{1}{N_c} \sum_{k=0}^{N_c-1} \alpha_m(k) \left[\sum_{\substack{\tau=0 \\ \tau \neq t}}^{N_c-1} s_m(\tau) \exp\left(j2\pi k \frac{t-\tau}{N_c} \right) \right] \right\} \\ \mu_{\mathrm{AWGN}} = \frac{1}{SF} \sum_{t=nSF}^{(n+1)SF-1} \left\{ c^*_m(t) \times \frac{1}{\sqrt{N_c}} \sum_{k=0}^{N_c-1} \hat{\Pi}_m(k) \exp\left(j2\pi t \frac{k}{N_c} \right) \right\} \end{cases} \quad (31)$$

where we have (33), shown at the bottom of the page, for the given set of $\{H_m(k)$ and $H_{m-1}(k);\ k=0\sim(N_c-1)\}$. The substitution of (28) and (33) into (32) gives

$$\sigma_\mu^2=\frac{1}{SF}\frac{N_0}{T_c}\left[\frac{1}{N_c}\sum_{k=0}^{N_c-1}|w_m(k)|^2+\left(\frac{E_c}{N_0}\right)\left\{\frac{1}{N_c}\sum_{k=0}^{N_c-1}|w_m(k)H_m(k)|^2-\left|\frac{1}{N_c}\sum_{k=0}^{N_c-1}w_m(k)H_m(k)\frac{T_{m-1}(k)}{|T_{m-1}(k)|}\right|^2\right\}\right]. \quad (34)$$

In the following analysis, an expression is derived for the approximate conditional BER. Incorrect decision feedback produces the error propagation. An exact BER analysis taking into account the error propagation is very difficult, if not impossible. First, we derive the approximate conditional BER due to the AWGN plus ICI, assuming no noise contribution in the reference signal $\hat{X}_{m-1}(k)$ like (23). Then, we obtain the approximate conditional BER taking into account the error propagation due to decision feedback. We assume QPSK data modulation and assume all "1" transmission (i.e., $d(n)=(1+j1)/\sqrt{2}$) without loss of generality. Since ICI can be assumed to be circularly symmetric, the conditional BER due to the AWGN plus ICI for the given set of $\{H_m(k)$ and $H_{m-1}(k);\ k=0\sim(N_c-1)\}$ can be expressed as

$$\begin{aligned}p_{b,\mathrm{AWGN+ICI}}&\left(\frac{E_s}{N_0},\{H_m(k),H_{m-1}(k)\}\right)\\&=\mathrm{Prob}\left[\mathrm{Re}[\hat{d}(n)]<0\,|\{H_m(k),H_{m-1}(k)\}\right]\\&=\frac{1}{2}erfc\left[\frac{\mathrm{Re}\left[\left(\frac{1}{N_c}\sum_{k=0}^{N_c-1}\alpha_m(k)\right)\frac{1+j1}{\sqrt{2}}\right]}{\sqrt{2}\sigma_\mu}\right]\end{aligned} \quad (35)$$

where $erfc[x]=(2/\sqrt{\pi})\int_x^\infty\exp(-t^2)dt$ is the complementary error function and we have (36), as shown at the bottom of the page, where $E_s/N_0=SF(E_c/N_0)$ is the average symbol energy-to-AWGN power spectrum density ratio. Assuming a very slow fading and perfect decision feedback as in (23), we have

$$\hat{X}_{m-1}(k)\to\sqrt{\frac{2E_c}{T_c}}\left(\frac{T_{m-1}(k)}{|T_{m-1}(k)|}\right)H_{m-1}(k). \quad (37)$$

Then, the FDDDE weight $w_m(k)$ is given by

$$w_m(k)=\frac{H_{m-1}^*(k)\frac{T_{m-1}^*(k)}{|T_{m-1}(k)|}}{|H_{m-1}(k)|^2+\beta} \quad (38)$$

with $\beta=0$ for ZF and $\beta=SF(E_s/N_0)^{-1}$ for MMSE. Substituting (38) into (36) and using (35), the approximate conditional BER due to the AWGN plus ICI is obtained.

However, feeding back the past-detected symbols causes error propagation [22],[23]. According to [23], once a decision error is produced due to the AWGN plus ICI, the next decision error is most likely incorrect, but the decision error may not propagate further. In DS-CDMA with FDDDE using decision feedback, the detected symbol sequence of the $(m-1)$th block is respread to generate the chip sequence replica for obtaining $\{\tilde{S}_{m-1}(k);k=0\sim(N_c-1)\}$. Hence, a symbol error produced by the AWGN plus ICI is spread over all subcarriers. As a consequence, a decision error produced in the $(m-1)$th block likely results in N_c/SF symbol errors in the mth block. Therefore, the approximate conditional BER, taking into account the error propagation, is given by

$$P_b\left(\frac{E_s}{N_0}\right)\approx\left(1+\frac{N_c}{SF}\right)\times p_{b,\mathrm{AWGN+ICI}}\left(\frac{E_s}{N_0},\{H_m(k),H_{m-1}(k)\}\right). \quad (39)$$

The approximate average BER can be numerically evaluated by averaging (39) over $\{H_m(k)$ and $H_{m-1}(k);\ k=0\sim(N_c-1)\}$.

$$\begin{cases}\sigma_{\mathrm{ICI}}^2=\frac{1}{2}E[|\mu_{\mathrm{ICI}}|^2]=\frac{1}{2}\frac{1}{SF}\left[\frac{1}{N_c}\sum_{k=0}^{N_c-1}|\alpha_m(k)|^2-\left|\frac{1}{N_c}\sum_{k=0}^{N_c-1}\alpha_m(k)\right|^2\right]\\ \sigma_{\mathrm{AWGN}}^2=\frac{1}{2}E[|\mu_{\mathrm{AWGN}}|^2]=\frac{1}{SF}\frac{N_0}{T_c}\left(\frac{1}{N_c}\sum_{k=0}^{N_c-1}|w_m(k)|^2\right)\end{cases} \quad (33)$$

$$\begin{aligned}&\frac{\mathrm{Re}\left[\left(\frac{1}{N_c}\sum_{k=0}^{N_c-1}\alpha_m(k)\right)\frac{1+j1}{\sqrt{2}}\right]}{\sqrt{2}\sigma_\mu}\\&=\sqrt{\frac{1}{2}\left(\frac{E_s}{N_0}\right)}\frac{\mathrm{Re}\left\{\frac{1}{N_c}\sum_{k=0}^{N_c-1}w_m(k)H_m(k)\frac{T_{m-1}(k)}{|T_{m-1}(k)|}\right\}-\mathrm{Im}\left\{\frac{1}{N_c}\sum_{k=0}^{N_c-1}w_m(k)H_m(k)\frac{T_{m-1}(k)}{|T_{m-1}(k)|}\right\}}{\sqrt{\frac{1}{N_c}\sum_{k=0}^{N_c-1}|w_m(k)|^2+\frac{1}{SF}\left(\frac{E_s}{N_0}\right)\left\{\frac{1}{N_c}\sum_{k=0}^{N_c-1}|w_m(k)H_m(k)|^2-\left|\frac{1}{N_c}\sum_{k=0}^{N_c-1}w_m(k)H_m(k)\frac{T_{m-1}(k)}{|T_{m-1}(k)|}\right|^2\right\}}}\end{aligned} \quad (36)$$

TABLE I
SIMULATION CONDITIONS

Access scheme	DS-CMDA	MC-CDMA
Block Length	N_c=256	
Guard interval	N_g=32	
Data modulation	QPSK	
Rayleigh channel	L=16, $E[\lvert h_{m,l}\rvert^2]=1/L$ $\tau_l = l$, $\max_l\{\tau_l\} \le (N_g - 1)$	
Spreading code	Long Gold sequences	
Spreading Factor	SF=8, 16, 64	
Equalization schemes	MMSE-FDDDE, ZF-FDDDE	

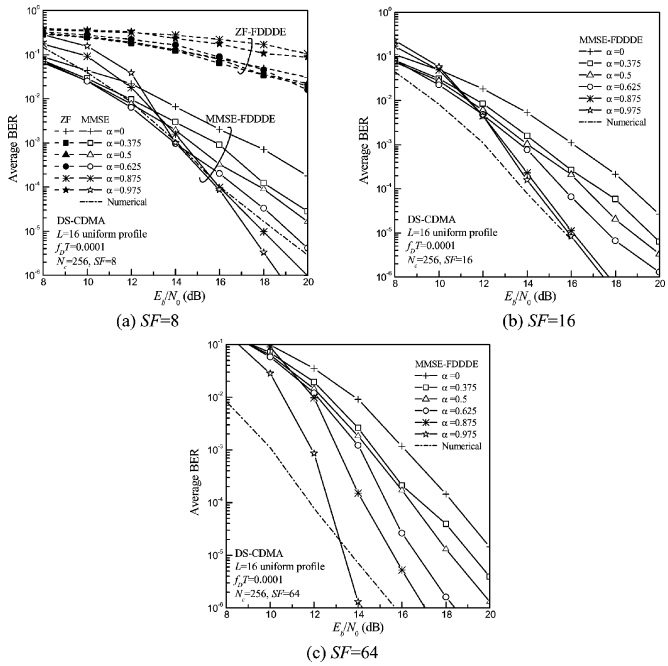

Fig. 2. Impact of forgetting factor α.

V. NUMERICAL AND SIMULATION RESULTS

The numerical and computer simulation conditions are shown in Table I. An L-path frequency-selective block Rayleigh fading channel having uniform power delay profile (i.e., $E[|h_{m,l}|^2] = 1/L$ for all m and l) is assumed. The lth path time delay τ_l is assumed to be $\tau_l = l$ chips and $\max_l\{\tau_l\} \le N_g - 1$. The numerical evaluation of the theoretical approximate BER is done by the Monte Carlo numerical computation method as follows. The set of path gains $\{h_{m,l}$ and $h_{m-1,l};\ l = 0 \sim L-1\}$ is generated to obtain $\{H_m(k)$ and $H_{m-1}(k);\ k = 0 \sim (N_c - 1)\}$ using (10) and then $\{w_m(k);\ k = 0 \sim (N_c - 1)\}$ using (38). The approximate conditional BER for the given average received E_s/N_0 is computed using (35) and (36). This is repeated a sufficient number of times to obtain the theoretical approximate average BER.

A. Impact of Forgetting Factor α of Decision Feedback IIR Filtering

The theoretical and computer simulated BER performances for FDDDE using ZF and MMSE are plotted in Fig. 2 for $SF = 8, 16$, and 64 as a function of the average received bit energy to the AWGN power spectrum density ratio E_b/N_0, which is defined as $E_b/N_0 = 0.5(E_s/N_0)(1 + N_g/N_c)$ for QPSK data modulation. $f_DT = 10^{-4}$ is assumed, where f_D is the maximum Doppler frequency and $T = (N_c + N_g)T_c$ is the block duration. First, a performance comparison between ZF- and MMSE-FDDDE is shown for $SF = 8$ in Fig. 2(a). ZF yields much worse performance than MMSE, similar to the case of coherent FDE [12]. It can be seen that, for MMSE-FDDDE, there is an optimum α that minimizes the BER at each E_b/N_0. For a smaller value of α, the noise reduction becomes less, but the tracking ability against fading increases. $\alpha = 0.625$ is shown to give an overall good BER performance over a wide range of E_b/N_0 values for $SF = 8$; while $\alpha = 0.875$ and 0.975 give an overall good BER performance for $SF = 16$ and 64, respectively. Although there is a gap between theoretical and computer simulation results, the simulated BER performance using suitable α is close to the theoretically predicted approximate BER performance. This validates our analysis of the conditional BER taking into account the error propagation. However, for large values of SF, there is a gap between the theoretical and computer simulation results. This is because the symbol energy is spread over a large number of chips resulting in low chip energy; therefore, the neglect of the noise contribution in $\hat{X}_{m-1}(k)$ leads to a large deviation of the approximate BER performance from the computer simulation results (for the approximate BER analysis in Section IV, the noise contribution in $\hat{X}_{m-1}(k)$ is neglected; meanwhile, in the computer simulation, the noise contribution in $\hat{X}_{m-1}(k)$ is considered).

B. Comparison With Pilot-Assisted Coherent FDE

The BER performance of MMSE-FDDDE is compared with that of coherent MMSE-FDE (no differential encoding is used) for different values of SF. As shown in Section V-A, the forgetting factor α that gives an overall good BER performance over a wide range of E_b/N_0 values was found to be $\alpha = 0.625, 0.875$, and 0.975 when $f_DT = 10^{-4}$ for $SF = 8, , 16$, and 64, respectively. Coherent FDE requires channel estimation. In the computer simulation, we use pilot-assisted channel estimation, where P pilot chip blocks are periodically transmitted, followed by $P \cdot D$ data chip blocks. The pilot-assisted channel estimation used in the computer simulation is described in Appendix A. The simulated BER performances of MMSE-FDDDE and coherent MMSE-FDE are plotted in Fig. 3. $(P, D) = (1, 15)$ and (4,15) are used for coherent MMSE-FDE. As P increases, the BER performance with coherent MMSE-FDE improves and approaches that of ideal channel estimation. Our proposed FDDDE can get close to coherent FDE with $(P, D) = (4, 15)$ and better than that with $(P, D) = (1, 15)$ for high E_b/N_0 values.

Fig. 4 shows the impact of the fading rate on the BERs achieved by MMSE-FDDDE and coherent MMSE-FDE for $E_b/N_0 = 18$ dB and $SF = 8$. $(P, D) = (1, 15), (4, 7)$, and $(4, 15)$ are used for coherent MMSE-FDE. It can be seen from Fig. 4 that as the f_DT value increases (or fading becomes faster), coherent FDE tends to lose the tracking ability, thereby resulting in significant performance degradation. Although FDDDE is inferior to coherent FDE for small f_DT values, it is superior for large f_DT values.

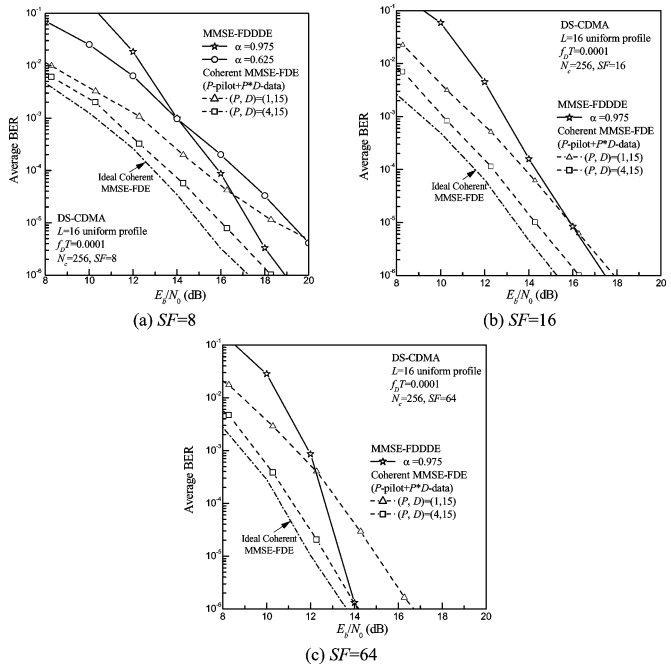

Fig. 3. Comparison between MMSE-FDDDE and coherent MMSE-FDE.

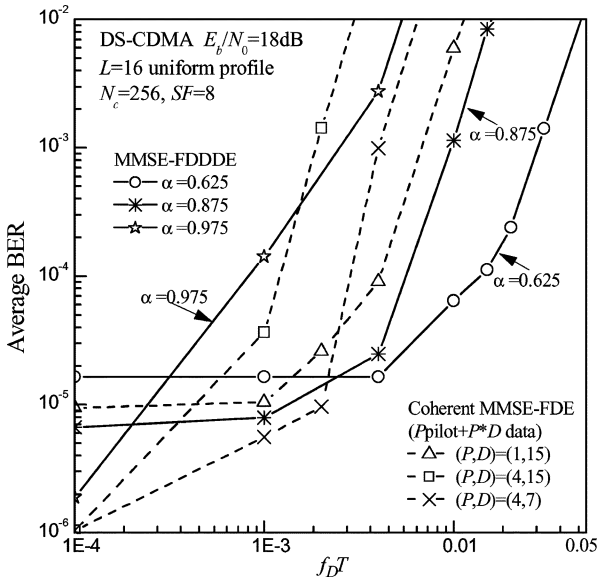

Fig. 4. Impact of fading rate.

C. Comparison With MC-CDMA

The proposed FDDDE can also be applied to differentially encoded MC-CDMA, which is described in Appendix B. The simulated BER performances of uncoded DS- and MC-CDMA both using MMSE-FDDDE are plotted in Fig. 5 for $f_DT = 10^{-4}$. It can be seen that, similar to coherent MMSE-FDE [12], DS-CDMA with MMSE-FDDDE achieves better BER performance than MC-CDMA with MMSE-FDDDE when $SF \ll N_c$. The reason for this is discussed as follows. Since, in DS-CDMA, each data symbol is always spread over all subcarriers, a full frequency-diversity effect can always be obtained, and hence a good BER performance is achieved irrespective of *SF*. However, the BER performance of MC-CDMA depends on *SF*. When $SF < N_c$,

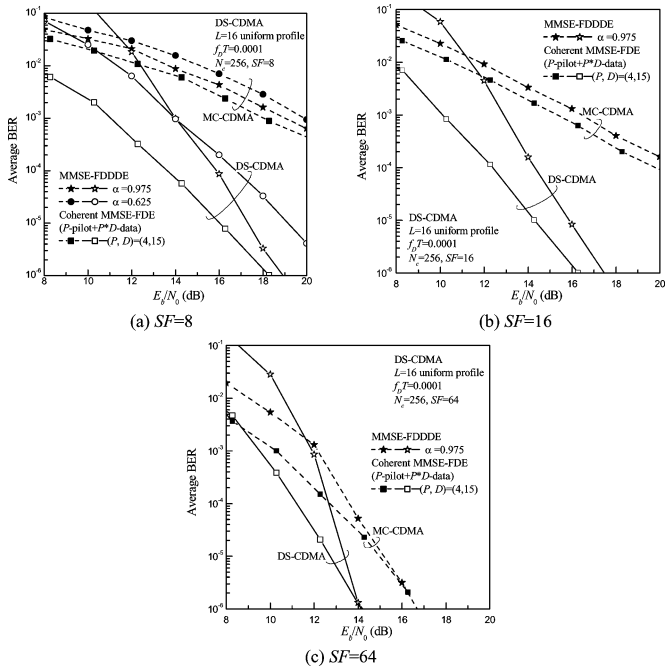

Fig. 5. Performance comparison between DS- and MC-CDMA.

in MC-CDMA, each data symbol is spread over fewer numbers of subcarriers, hence the frequency-diversity effect becomes smaller; therefore, the BER performance degrades and becomes inferior to that of DS-CDMA. However, when *SF* is equal to the number of subcarriers, the BER performance of MC-CDMA becomes the same as that of DS-CDMA, since the frequency-diversity effect can be fully exploited.

For comparison, the BER performance with coherent MMSE-FDE using $(P, D) = (4, 15)$ is also plotted in Fig. 5. Although MMSE-FDDDE is inferior to coherent MMSE-FDE, the BER with MMSE-FDDDE approaches that of coherent MMSE-FDE as the E_b/N_0 becomes larger for both DS- and MC-CDMA when $\alpha = 0.975$.

The DS-CDMA signal amplitude after frequency-domain differential encoding is not any more constant. Large amplitude fluctuations may appear in the transmitted signal waveform, similar to MC-CDMA. The statistical property of amplitude variations in terms of peak-to-average power ratio (PAPR) is investigated. The PAPR of the mth block transmitted signal $s_m(t)$ in (5) is defined as the ratio of the instantaneous peak power to the ensemble average power

$$\text{PAPR}_m = \frac{\max\{|s_m(t)|^2\}}{E[|s_m(t)|^2]} \tag{40}$$

for $t = 0 \sim (N_c - 1)$. The PAPR is a random variable. We measured the PAPRs of more than one million blocks and computed the probability distribution of the PAPR [24], [25]. The probability of PAPR exceeding a certain level is plotted in Fig. 6. It is seen that the frequency-domain differentially encoded DS-CDMA signal has almost the same PAPR distribution as MC-CDMA signal.

In this paper, we have shown that the differential encoding and detection can also be applied to DS-CDMA in a frequency-selective fading channel; however, this is only possible at the cost of increased PAPR.

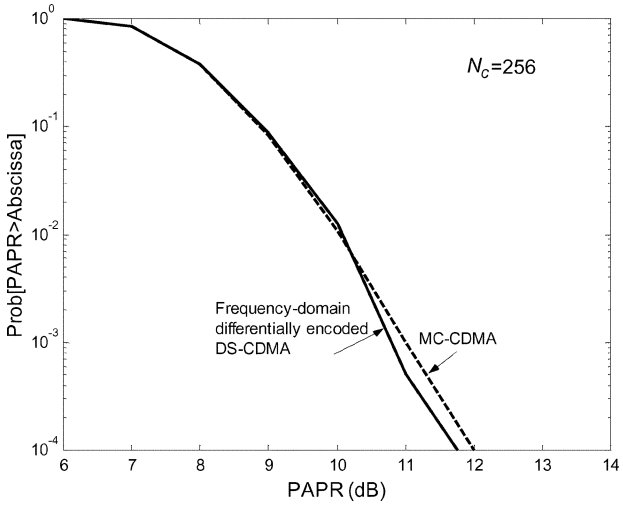

Fig. 6. PAPR comparison between MC- and DS-CDMA with FDDDE.

VI. Conclusion

In this paper, a frequency-domain differential encoding and detection was proposed for DS-CDMA signal transmission in a frequency-selective fading channel. Joint FDDDE based on MMSE criterion was presented. It was confirmed by the approximate BER analysis and computer simulation that the proposed MMSE-FDDDE is very robust against the Doppler spread and outperforms coherent MMSE-FDE for large Doppler spreads. The proposed FDDDE can also be applied to MC-CDMA. In this paper, we have considered uncoded DS- and MC-CDMA. The performance comparison between uncoded DS- and MC-CDMA, both using MMSE-FDDDE, has shown that DS-CDMA achieves better BER performance than MC-CDMA when $SF \ll N_c$, due to the larger frequency-diversity effect of DS-CDMA. Channel coding can improve significantly the BER performance for both DS- and MC-CDMA. The coding gain for both systems may depend on the modulation level (e.g., QPSK, 16QAM, and 64QAM), channel frequency-selectivity, etc. [27]. Performance analysis of coded DS- and MC-CDMA with higher level modulation is an important issue and is left as an interesting future study.

In this paper, the BER performance of the single user case was only evaluated. Based on the Gaussian approximation of the multiuser interference (MUI), the BER performance in a multiuser environment can be predicted using the BER performance of the single user case (see Appendix C). However, the Gaussian approximation of the MUI becomes inaccurate as the number of users becomes small. We would like to leave the detailed performance analysis in a multiuser environment for a future study.

Appendix A
Pilot-Assisted Channel Estimation for Coherent FDE

For pilot-assisted channel estimation, P pilot chip blocks are periodically transmitted every $P \cdot D$ data chip blocks. The initial channel estimate $\hat{H}_m(k)$ can be obtained by removing the pilot modulation from $R_m(k)$. This is done by multiplying $R_m(k)$ with the complex conjugate of pilot subcarrier component $P_m(k)$, i.e., $\hat{H}_m(k) = R_m(k)P_m^*(k)$. However, $\hat{H}_m(k)$ is perturbed by the AWGN. To suppress the noise, the delay-time domain windowing technique [15], [16] is applied. Here, the N_c-point IFFT is first applied to noisy estimate $\hat{H}_m(k)$ to obtain the noisy channel impulse response $\hat{h}_m(\tau)$. In general, the number of paths and their time delays are unknown to the receiver. The GI is set such that the channel impulse response $h_m(\tau)$ is present only within the GI length, but the noise due to the AWGN is present over the entire range, so the noise effect can be suppressed by replacing $\hat{h}_m(\tau)$ beyond the GI with zero (or zero padding). Then, after applying N_c-point FFT, the improved estimate $\widetilde{H}_m(k)$ is obtained, where $m = 0 \sim (P-1)$. Further improved channel estimation can be achieved by averaging P estimates as follows:

$$\overline{H}(k) = \frac{1}{P}\sum_{m=0}^{P-1} \widetilde{H}_m(k). \tag{A1}$$

The coherent FDE weight is given by

$$w(k) = \frac{\overline{H}^*(k)}{\left|\overline{H}(k)\right|^2 + \beta} \tag{A2}$$

with $\beta = 0$ for ZF and $\beta = SF(E_s/N_0)^{-1}$ for MMSE. $w(k)$ is used for coherent FDE of the mth block when $m = P \sim P(1+D) - 1$. With decreasing D, the tracking ability against fading improves, but the energy loss due to the insertion of pilot chip blocks, given by $10\log(1+D)/D$ dB, becomes larger.

Appendix B
FDDDE for Differentially Encoded MC-CDMA

Assuming QPSK data modulation, the mth block symbol sequence $b_m(n)$ is spread by the spreading sequence $c_m(t)$, with $|b_m(n)| = |c_m(t)| = 1$. The resultant mth block spread chip sequence $d_m(t)$ can be expressed as

$$d_m^{MC}(t) = b_m^{MC}\left(\left\lfloor \frac{t}{SF} \right\rfloor\right) c_m(t). \tag{B1}$$

After serial-to-parallel transmission, block-by-block frequency-domain differential encoding at the kth subcarrier is performed at a transmitter as

$$T_m^{MC}(k) = d_m^{MC}(k) T_{m-1}^{MC}(k) \tag{B2}$$

with $m \geq 1$ and $k = 0 \sim (N_c - 1)$, where we assume that the same FFT block size N_c is used for both DS- and MC-CDMA. $T_m(k)$ is the differentially encoded subcarrier component with $|T_m(k)| = 1$. At $m = 0$, the reference chip block $T_0(k)$ needed to be transmitted

At a receiver, the kth subcarrier component $R_m^{MC}(k)$ of the received mth block MC-CDMA signal can be expressed as

$$R_m^{MC}(k) = \sqrt{\frac{2E_c}{T_c}} H_m(k) T_m^{MC}(k) + \Pi_m(k) \tag{B3}$$

where E_c is the signal energy per FFT (or IFFT) sample and T_c is the FFT sample period. Subcarrier-by-subcarrier FDDDE in MC-CDMA is carried out as

$$\hat{d}_m^{MC}(k) = w_m^{MC}(k) R_m^{MC}(k) \tag{B4}$$

where $w_m^{MC}(k)$ is the FDDDE weight and is given by

$$w_m^{MC}(k) = \frac{\hat{R}_{m-1}^{MC*}(k)}{\left|\hat{R}_{m-1}^{MC}(k)\right|^2 + \beta} \tag{B5}$$

with $\beta = 0$ for ZF and $\beta = SF(E_s/N_0)^{-1}$ for MMSE. Similar to DS-CDMA, $\hat{R}_{m-1}^{MC}(k)$ is the output of the decision feedback IIR filter, given by

$$\hat{R}_{m-1}^{MC}(k) = \alpha \hat{R}_{m-2}^{MC}(k)\tilde{d}_{m-1}(k) + (1-\alpha)R_{m-1}^{MC}(k) \tag{B6}$$

for $m \geq 2$, where $\hat{R}_0^{MC}(k) = R_0^{MC}(k)$ is the received reference signal. Next, the despreading operation is performed in the frequency domain. The decision variable $\hat{b}^{MC}(k)$ is given by

$$\begin{aligned}\hat{b}^{MC}(n) &= \frac{1}{SF}\sum_{k=nSF}^{(n+1)SF-1} \hat{d}_m^{MC}(k)c_m^*(k) \\ &= \left(\frac{1}{SF}\sum_{k=nSF}^{(n+1)SF-1} \alpha_m^{MC}(k)\right)b_m(n) + \mu_{\text{AWGN}}^{MC}\end{aligned} \tag{B7}$$

where

$$\alpha_m^{MC}(k) = \sqrt{\frac{2E_c}{T_c}}w_m^{MC}(k)H_m(k)T_{m-1}(k). \tag{B8}$$

The variance of μ_{AWGN}^{MC} is given by

$$2\left(\sigma_\mu^{MC}\right)^2 = \frac{2N_0}{T_c}\frac{1}{SF^2}\sum_{k=nSF}^{(n+1)SF-1}\left|w_m^{MC}(k)\right|^2. \tag{B9}$$

In the following, an approximate conditional BER taking into account the decision feedback is derived. Assuming the perfect decision feedback and no noise contribution, we have

$$\hat{X}_{m-1}^{MC}(k) \to \sqrt{\frac{2E_c}{T_c}}T_{m-1}(k)H_{m-1}(k) \text{ as } \alpha \to 1. \tag{B10}$$

Therefore, the FDDDE weight is given by

$$w_m^{MC}(k) = \frac{H_{m-1}^*(k)T_{m-1}^*(k)}{|H_{m-1}(k)|^2 + \beta}. \tag{B11}$$

The approximate conditional BER due to the AWGN for MC-CDMA, corresponding to (34) for DS-CDMA, is given by

$$\begin{aligned}&p_{b,\text{AWGN}}^{MC}\left(\frac{E_s}{N_0}, \{H_m(k), H_{m-1}(k)\}\right) \\ &= \frac{1}{2}erfc\left[\frac{\text{Re}\left[\left(\frac{1}{SF}\sum_{k=nSF}^{(n+1)SF-1}\alpha_m^{MC}(k)\right)\frac{1+j1}{\sqrt{2}}\right]}{\sqrt{2}\sigma_\mu^{MC}}\right]\end{aligned} \tag{B12}$$

where we obtain (B13), shown at the bottom of the page. Due to the employment of decision feedback IIR filtering, decision error in the previous block causes error propagation. In DS-CDMA, a decision error spreads over all subcarriers, while in MC-CDMA, subcarriers belonging to the data symbol in error are only affected. Therefore, double symbol errors are likely produced when decision feedback filtering is used [22], [23]. Therefore, substituting (B11) into (B13) and using (B12), the approximate conditional BER of MC-CDMA is given by

$$P_b^{MC}\left(\frac{E_s}{N_0}\right) = 2 \times p_{b,\text{AWGN}}^{MC}\left(\frac{E_s}{N_0}, \{H_m(k), H_{m-1}(k)\}\right). \tag{B14}$$

The approximate average BER can be numerically evaluated by averaging (B14) over $\{H_m(k)$ and $H_{m-1}(k);\ k = 0 \sim (N_c - 1)\}$.

Appendix C
Prediction of BER Performance in a Multiuser Environment

In the case of uplink (mobile-to-base station), the differentially encoded DS-CDMA signals of different users pass through different frequency-selective channels and the sum of different users' signals and the noise due to AWGN is received at a base station. Thereby, the resulting multiuser interference (MUI) degrades the BER performance. The BER performance in the presence of MUI can be predicted using the BER performance of the single user case obtained in this paper. For a large number of users, the MUI from multiple users can be approximated as a Gaussian noise according to the central limit theorem. Hence, the sum of MUI and the noise can be treated as a new complex Gaussian noise [26]. The MUI plus noise power spectrum density η_0 is given by

$$\eta_0 = N_0 + (U-1)\frac{2E_b}{SF} = N_0\left[1 + \frac{U-1}{\frac{SF}{2}}\frac{E_b}{N_0}\right] \tag{C1}$$

for QPSK data modulation, where N_0 is the AWGN, E_b is the bit energy, and U is the number of active users. The signal energy-to-MUI plus noise power spectrum density ratio is given by

$$\frac{E_b}{\eta_0} = \frac{E_b}{N_0}\left[1 + \frac{U-1}{\frac{SF}{2}}\frac{E_b}{N_0}\right]. \tag{C2}$$

Accordingly, the BER at $E_b/N_0 = \Gamma$ in a multiuser environment can be approximately given by the BER at $E_b/N_0 =$

$$\begin{aligned}&\frac{\text{Re}\left[\left(\frac{1}{SF}\sum_{k=nSF}^{(n+1)SF-1}\alpha_m^{MC}(k)\right)\frac{1+j1}{\sqrt{2}}\right]}{\sqrt{2}\sigma_\mu^{MC}} \\ &= \sqrt{\frac{1}{2}\left(\frac{E_s}{N_0}\right)}\frac{\text{Re}\left\{\frac{1}{SF}\sum_{k=nSF}^{(n+1)SF-1}w_m^{MC}(k)H_m(k)T_{m-1}(k)\right\} - \text{Im}\left\{\frac{1}{SF}\sum_{k=nSF}^{(n+1)SF-1}w_m^{MC}(k)H_m(k)T_{m-1}(k)\right\}}{\sqrt{\frac{1}{SF}\sum_{k=nSF}^{(n+1)SF-1}\left|w_m^{MC}(k)\right|^2}}\end{aligned} \tag{B13}$$

$\Gamma/[1+\Gamma(U-1)/(SF/2)]$ in the single user case. Therefore, based on the Gaussian approximation of the MUI, we can predict the BER performance in a multiuser environment using our simulation results in the paper. However, if U becomes small, the Gaussian approximation of MUI becomes inaccurate and the predicted BER performance may deviate from the exact performance.

REFERENCES

[1] F. Adachi, "Wireless past and future-evolving mobile communications systems," *IEICE Trans. Fundamentals*, vol. E84-A, no. 1, pp. 55–60, Jan. 2001.

[2] W. C. Jakes, *Microwave Mobile Communications*, W. C. Jakes, Jr., Ed. New York: Wiley, 1974.

[3] J. G. Proakis, *Digital Communications*, 2nd ed. New York: McGraw-Hill, 1995.

[4] A. J. Viterbi, *CDMA: Principles of Spread Spectrum Communications*. Reading, MA: Addison-Wesley, 1995.

[5] F. Adachi, M. Sawahashi, and H. Suda, "Wideband DS-CDMA for next generation mobile communications systems," *IEEE Commun. Mag.*, vol. 36, no. 9, pp. 56–69, Sep. 1998.

[6] S. Hara and R. Prasad, "Overview of multicarrier CDMA," *IEEE Commun. Mag.*, vol. 35, no. 12, pp. 126–144, Dec. 1997.

[7] ——, *Multicarrier Techniques for 4G Mobile Communications*. Boston, MA: Artech, 2003.

[8] R. Van Nee and R. Prasad, *OFDM for Wireless Multimedia Communications*. Boston, MA: Artech, 2000.

[9] N. Yee, J.-P. Linnarts, and G. Fettweis, "Multi-carrier CDMA in indoor wireless radio networks," in *Proc. PIMRC*, May 1993, pp. 109–113.

[10] D. Falconer, S. L. Ariyavisitakul, A. Benyamin -Seeyar, and B. Eidson, "Frequency domain equalization for single-carrier broadband wireless systems," *IEEE Commun. Mag.*, vol. 40, no. 4, pp. 58–66, Apr. 2002.

[11] F. Adachi, T. Sao, and T. Itagaki, "Performance of multicode DS-CDMA using frequency domain equalization in frequency-selective fading channel," *Electron. Lett.*, vol. 39, no. 2, pp. 239–241, Jan. 2003.

[12] F. Adachi and K. Takeda, "Bit error rate analysis of DS-CDMA with joint frequency-domain equalization and antenna diversity combining," *IEICE Trans. Commun.*, vol. E87-B, no. 10, pp. 2991–3002, Oct. 2004.

[13] A. Chouly, A. Brajal, and S. Jourdan, "Orthogonal multicarrier techniques applied to direct sequence spread spectrum CDMA system," in *Proc. IEEE GLOBECOM*, vol. 2, Nov. 2003, pp. 1723–1728.

[14] D. N. Kalofonos, M. Stojanovic, and J. G. Proakis, "Performance of adaptive MC-CDMA detectors in rapidly fading Rayleigh channels," *IEEE Trans. Wireless Commun.*, vol. 2, no. 2, pp. 229–239, Mar. 2003.

[15] J.-J. van de Beek, O. Edfors, M. Sandell, S. K. Wilson, and P. O. Borjesson, "On channel estimation in OFDM systems," in *Proc. Veh. Technol. Conf.*, Chicago, IL, Jul. 1995, pp. 815–819.

[16] T. Fukuhara, H. Yuan, Y. Takeuchi, and H. Kobayashi, "A novel channel estimation method for OFDM transmission technique under fast time-variant fading channel," in *Proc. Veh. Technol. Conf.-Spring*, Jeju, Korea, Apr. 2003, pp. 2343–2347.

[17] D. Falconer, S. L. Ariyavisitakul, A. Benyamin-Seeyar, and B. Eidson, "Frequency domain equalization for single-carrier broadband wireless systems," *IEEE Commun. Mag.*, vol. 40, no. 4, pp. 58–66, Apr. 2002.

[18] T. S. Rappaport, *Wireless Communications*. Englewood Cliffs, NJ: Prentice–Hall, 1996.

[19] S. Haykin, *Adaptive Filter Theory*. Englewood Cliffs, NJ: Prentice-Hall, 1991.

[20] B. Widrow and S. Stearns, *Adaptive Signal Processings*. Englewood Cliffs, NJ: Prentice-Hall, 1985.

[21] J. G. Proakis and D. G. Manolakis, *Digital Signal Processing*. Englewood Cliffs, NJ: Prentice–Hall, 1996.

[22] F. Adachi and M. Sawahashi, "Decision feedback multiple-symbol differential detection for M-ary DPSK," *Electron. Lett.*, pp. 1385–1387, Jul. 1993.

[23] F. Adachi, "Reduced-state Viterbi differential detection using a recursively estimated phase reference for M-ary DPSK," *Inst. Elec. Eng. Proc. Commun.*, vol. 142, pp. 263–270, Aug. 1995.

[24] X. K. Zhao and X. D. Zhang, "Peak-to-average power ratio analysis in multicarrier DS-CDMA," *IEEE Trans. Veh. Technol.*, vol. 52, no. 3, pp. 561–568, May 2003.

[25] P. Boonsrimuang, K. Mori, T. Paungma, and H. Kobayashi, "Proposal of clipping and inter-modulation noise mitigation method for OFDM signal in nonlinear channel," *IEICE Trans. Commun.*, vol. E88-B, no. 2, pp. 427–435, Feb. 2005.

[26] K. K. Duk and F. Adachi, "Theoretical analysis of reverse link capacity for an SIR-based power-controlled cellular CDMA system in a multi-path fading environment," *IEEE Trans. Veh. Technol.*, vol. 50, no. 2, pp. 452–464, Mar. 2001.

[27] F. Adachi, D. Garg, S. Takaoka, and K. Takeda, "Broadband CDMA techniques," *IEEE Wireless Commun. Mag.*, vol. 2, no. 2, pp. 2–13, Apr. 2005.

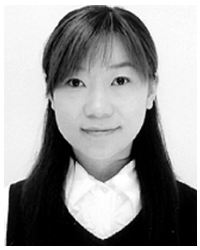

Le Liu (S'05) received the B.S. and M.S. degrees in electrical engineering from Beijing University of Posts and Telecommunications (BUPT), Beijing, China, in 2000 and 2003, respectively. Currently, she is working towards the Ph.D. degree in the Department of Electrical and Communication Engineering, Graduate School of Engineering, Tohoku University, Sendai, Japan, with a scholarship from the Japanese government.

From April 2003 to September 2004, she took part in the collaboration between the National Institute of Information and Communications Technology (NICT), Japan, and BUPT on the 4G Wireless Telecommunications Project. Her research interests include digital signal transmission techniques for direct sequence CDMA and multicarrier CDMA.

Fumiyuki Adachi (M'79–SM'90–F'00) received the B.S. and Dr. Eng. degrees in electrical engineering from Tohoku University, Sendai, Japan, in 1973 and 1984, respectively.

In April 1973, he joined the Electrical Communications Laboratories of Nippon Telegraph & Telephone Corporation (now NTT) and conducted various types of research related to digital cellular mobile communications. From July 1992 to December 1999, he was with NTT Mobile Communications Network, Inc. (now NTT DoCoMo, Inc.), where he led a research group on wideband/broadband CDMA wireless access for IMT-2000 and beyond. Since January 2000, he has been with Tohoku University, where he is a Professor of Electrical and Communication Engineering at the Graduate School of Engineering. From October 1984 to September 1985, he was a U.K. SERC Visiting Research Fellow in the Department of Electrical Engineering and Electronics, Liverpool University. His research interests include CDMA wireless access techniques, equalization, transmit/receive antenna diversity, MIMO, adaptive transmission, and channel coding, with particular applications to broadband wireless communications systems.

Dr. Adachi is a member of the Institute of Electronics, Information and Communication Engineers of Japan (IEICE). He was a corecipient of the IEEE Vehicular Technology Transactions Best Paper of the Year Award, in 1980 and again in 1990, and also a recipient of the Avant Garde Award in 2000. He was a recipient of the IEICE Achievement Award in 2002, and a corecipient of the IEICE Transactions Best Paper of the Year Award in 1996 and again in 1998. He was a recipient of the Thomson Scientific Research Front Award 2004. He served as a Guest Editor of the IEEE JOURNAL ON SELECTED AREAS IN COMMUNICATIONS (Special Issues on Broadband Wireless Techniques, October 1999, Wideband CDMA I, August 2000, and Wideband CDMA II, January 2001).